



## ENGINEERING ASSESSMENTS OF LIQUEFACTION POTENTIAL OF BAGHDAD SOIL UNDER DYNAMIC LOADING

\*Dr. Bushra Suhail Albusoda

Assist Prof., Civil Engineering Department, Baghdad University, Baghdad, Iraq.

(Received: 1/9/2015 ; Accepted: 1/11/2015)

**Abstract:** This study is focused on the evaluation of liquefaction of Baghdad soil. Seven sites have been chosen along Tigris River. Various procedures were followed to evaluate liquefaction susceptibility of Baghdad soil. The variation of safety factor with depth had been investigated. The liquefaction-induced lateral spreading and settlement had been studied. The study revealed that the NCEER, 1997 workshop procedure is recommended for assessment of liquefaction of Baghdad soil while the Japanese highway bridge method is not convenient. A new proposed chart for preliminary assessment of liquefaction for Baghdad soil had been developed. This chart will be helpful in saving cost and time in liquefaction assessment of Baghdad soil.

**Keywords:** Baghdad soil, Liquefaction, Seismic analysis, Lateral Spreading.

### التقييم الهندسي للتسييل المحتمل لترربة بغداد تحت التحميل الديناميكي

**الخلاصة:** تركز هذه الدراسة على تقييم التسييل لترربة بغداد. تم اختبار سبعة مواقع محاذية لنهر دجلة لتقييم قابلية ترربة بغداد للتسييل باستخدام طرق مختلفة. تم تحري اختلاف عامل الأمان مع العمق ودراسة الانتشار الجانبي والهبوط الذي يسببه التسييل. كشفت الدراسة أنه من المستحسن اعتماد طريقة NCEER, 1997 workshop لتقييم التسييل لترربة بغداد في حين أن طريقة Japanese highway bridge غير ملائمة. تم استحداث مرسوم جديد مقترح لتقييم تسييل ترربة بغداد بشكل اولي. هذا المرسوم سيكون مفيداً في توفير التكاليف والوقت في تقييم تسييل ترربة بغداد.

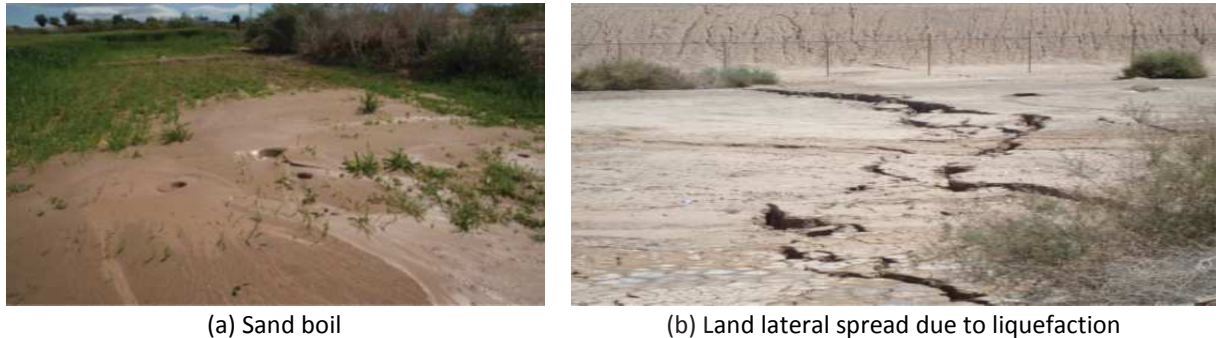
### 1. Introduction

The natural disasters have their socio-economic impact on the civil communities. The infrastructure is usually the most vulnerable to disasters in particular roads, bridges, dams, transit and aviation systems, schools, navigable waterways, energy resources, drinking water and solid and hazardous waste, [1].

Liquefaction can be one of factors which damage or destroy the structures built on the loose and saturated deposits. Liquefaction refers to the response of soil against dynamic loads (like earthquakes, subsurface blasting, pile driving, and vibrations from train traffic or transitional shearing waves) and then decrease part or all of resistance of the soil and the soil becomes liquefy. During ground shaking, shrinkage of pore spaces of loose to medium-compact granular soils squeezes the pore water; when the pore water cannot easily drain, the pore-water pressure, significantly increases, thus

\*[Dr.Bushra\\_albusoda@coeng.uobaghdad.edu.iq](mailto:Dr.Bushra_albusoda@coeng.uobaghdad.edu.iq)

reducing the effective stress, [1]. The soil loses grain-to-grain contact and tends to behave like a liquid. Liquefaction may cause the reduction or loss of bearing capacity, large settlement, and horizontal displacement because of lateral spreads of liquefied soils. Liquefaction can be exhibited in the forms of sand boils or lateral spread of surficial soils (Fig. 1), [2]. Examples of this type of damage were observed in many earthquakes, such as the 1964 Niigata, the 1964 Alaska, the 1971 San Fernando, the 1985 Mexico City, the 1994 Northridge, the 1994 Kobe, the 1999 Taiwan, the 1999 Turkey, the 2010 Baja California, and the 2011 Tohoku earthquakes.



(a) Sand boil

(b) Land lateral spread due to liquefaction

Figure 1. Liquefaction in the 2010 Baja California earthquake, Mw=7.2,[2]

## 2. Seismic Hazards in Iraq

Tectonically Iraq is located in a relatively active seismic zone at the northeastern boundaries of the Arabian Plate. This plate is moving toward the Turkish and Iranian plates counter-clockwise, and as a result of these collisions stresses occur is higher than the carrying rocks what happens break in the rocks, resulting in liberation of energy and this energy is spread in the form of waves in all directions, lead to vibrations. The corresponding Zagros, Tauros Belts manifest the subduction of the Arabian plate into the Iranian and Anatolian Plates .The seismic history reveals annual seismic activity of different strength. The territory of Iraq, although not directly located on a dense cluster of recent earthquake epicenters; but the geodynamic configurations show a medium to high seismic risk. This will be coupled with the increasing vulnerability of the major highly populated cities, [1],[3].

The north and northeastern zones depicts the highest seismic activity with strong diminution in the south and southwestern parts of the country. Fig. 2 represents a seismic acceleration map of Iraq, in which it is obvious that regions east of Tigris River have a seismic acceleration (greater than 0.2g) with magnitude  $M \geq 4.0$ , [4], [5]. The region between Tigris and Euphrates Rivers experiences a lower acceleration (0.1-0.2g). The seismic hazard near the source boundaries is directly and strongly affected by the change in the delineation of these boundaries. The forces which have formed the geological structure along the plate boundary in E and NE Iraq are still active causing stress and strain accumulation, and deformation. Highly destructive earthquake can be expected to occur in the future, [5].

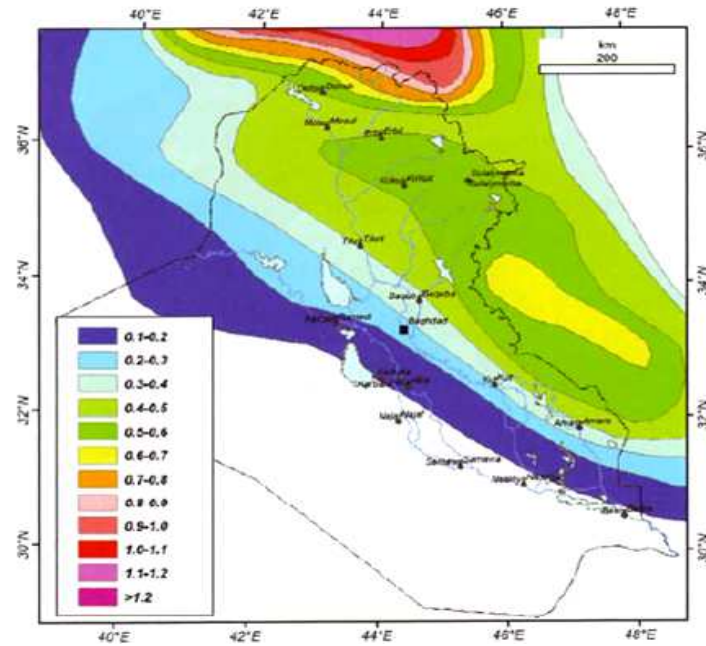


Figure 2. Seismic acceleration map with period of 100 years, [4]

From the previous discussion it can be found that, although Iraq is seemingly secure from seismic hazards, seismic observations indicate otherwise. Earthquakes are likely to happen and may cause substantial damage, especially in NE Iraq and in the Mesopotamian Plain due to Liquefaction or Quaternary sediments. It is therefore important to take into consideration seismic parameters in future design of large buildings. The last seismic event that takes place on November 23, 2013 confirmed this conclusion. The Iraqi seismic monitoring center\* declares, on Saturday November 23, 2013, that the number of earthquakes that hit different parts of Iraq amounted to more than 50 earthquakes. The number of major earthquakes that hit central, northern and southern areas of Iraq were four of the most powerful occurred in the ninth hour and 31 minutes and was measuring 5.6 according to Richter scale and depth of up to 17 km, and its east Khanaqin in Diyala province and that felt by the people of Baghdad and was followed by more than 50 aftershocks between tangible and non-tangible attributing the cause of earthquakes in general to tectonic plate movement, and as Iraq is located on the north-east of the Arabian plate,[6].

### 3. Site Locations and Descriptions

Extensive borehole data were collected from various public and private organizations for seven sites in Baghdad. These sites have been chosen to evaluate their susceptibility to liquefaction. The sites distributed from northeast to south of Baghdad. Some of these sites are near Tigris River while the others somewhat far from the river. The locations of these sites could be shown in Fig. 3. Geologically, Baghdad lies within the Mesopotamian plain. Most of the Mesopotamian Plain is flat broad area. The Mesopotamian Zone was represents by the Quaternary Sediments that range in age from Pleistocene to Holocene, and in thickness from few meters up to 250 m, which were deposited by the interacting Tigris and Euphrates rivers, on the alluvial fans from the surrounding elevated areas, [4].

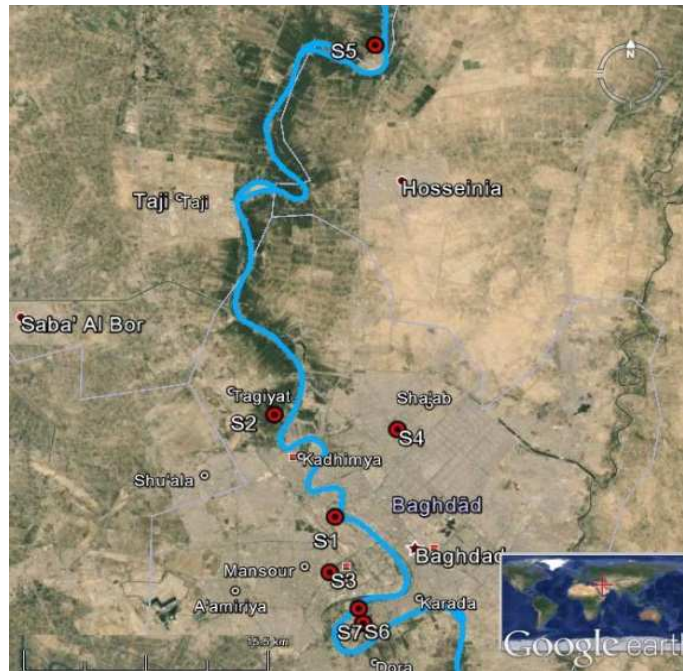


Figure 3.Sites Distribution on Baghdad Map (Google earth image)

Generally, the soil profiles for these sites are composed of clay layer followed by loose to medium silty sand to sand layer. Several geotechnical properties at different depths have been obtained for each site such as standard penetration number (N), fine contents, unit weight ( $\gamma_t$ ), undrained shear strength ( $S_u$ ) and ground water levels ( $Z_w$ ) as shown in Table 1. The maximum acceleration values ( $a_{max}$ ) shown in Table 1 are chosen based on the site location on the seismic acceleration map (shown in Fig. 2).

Table1.Geotechnical properties of soil for all sites under study

Site		H,m	SPT-N	$\gamma_t$ , kN/m <sup>3</sup>	Fines,%	D <sub>50</sub> ,mm	Z <sub>w</sub> ,m	S <sub>u</sub> ,kPa	a <sub>max</sub>
S1	Clay	6.5	7-9	18.5	80	0.002	2.2	40	(0.2-0.3)g
	Sand	13	12-25	17-19	18-19	0.2		-	
S2	Clay	4	6-10	18.5	85	0.002	0.8	35	(0.2-0.3)g
	Sand	13	11-29	17-19	11-28	0.3		-	
S3	Clay	8	34	21	94	0.003	1.4	150	(0.2-0.3)g
	Sand	4.5	6-12	19	94	0.004		-	
S4	Clay	8.5	12-20	19.5	98	0.002	1.4	45	(0.2-0.3)g
	Sand	18	7-34	18-19	10-27	0.1-0.2		-	
S5	Clay	2	18	16.5	85	0.002	3	60	(0.3-0.4)g
	Sand	19	15-41	16.5-19.5	8-16	0.02-0.2		-	
S6	Clay	2.5	18	18	88	0.002	3	35	(0.2-0.3)g
	Sand	23	15-37	16-19.5	8-16	0.1-0.2		-	
S7	Clay	3.5	6-8	18.5	85	0.002	3.5	25	(0.2-0.3)g
	Sand	17.5	8-32	17-18.5	13-21	0.1-0.25		-	

#### 4. Liquefaction Considerations

It is widely accepted that only recent sediments or fills of saturated, cohesionless soils at shallow depths will liquefy due to earthquake. The conditions required for liquefaction to occur are [2]:

- the soil deposit is sandy or silty soil;
- the soil is saturated or nearly saturated (usually below groundwater table);



- c. the soil is loose or medium compact;
- d. the soil is subjected to seismic stress (such as from earthquake, blast, etc.).

Dense granular soils are less likely to liquefy than looser soils. Granular soils under higher initial confining effective stress (e.g., deeper soils) are less likely to liquefy. Case histories indicate that liquefaction usually occurs within a depth of 15m. Cohesive soils are generally not susceptible to liquefaction. More quantitative assessments of liquefaction susceptibility are possible with information from subsurface soil explorations, [2].

#### 4. Evaluation of Liquefaction Potential

Liquefaction is commonly evaluated using a factor of safety which is defined as the ratio between the available liquefaction resistance, expressed in terms of the cyclic stresses required to cause liquefaction, and the cyclic stresses generated by the design earthquake (equation (1)). Both of these stress parameters are commonly normalized with respect to the effective overburden stress at the depth in question. They are referred to as cyclic resistance ratio (CRR) and cyclic stress ratio (CSR), [7].

$$FS = \frac{CRR_{7.5}}{CSR} * K_{\sigma} * K_{\alpha} \quad (1)$$

$K_{\sigma}$  is the overburden stress correction factor; only applied to the following analysis methods that adopted in this research:(NCEER [7] , Vancouver Task Force Report [8], Idriss and Boulanger [9]). Each of these methods has its own equation for calculating  $K_{\sigma}$ .  $K_{\alpha}$  is ground slope correction.

Seed and Idriss considered the soil layer with FS value between 1.25 and 1.5 as non-liquefiable, while soil layers with FS between 1.0 and 1.2 are defined as marginally liquefiable. The actual FS selected is based on the importance of the structure and the potential for ground displacement. In calculating the factor of safety, the empirical methods are most widely used in practice. Seed and Idriss [10] first developed and published the “simplified procedure” for evaluating liquefaction resistance. The NCEER workshop resulted in a milestone report, [7], [11], which is the most updated liquefaction evaluation reference to date, [2].The evaluations of CSR and CRR in the following sections are based on this report.

#### 5. Liquefaction Analysis

More quantitative assessments of liquefaction susceptibility are possible with information from subsurface soil explorations. Two basic approaches have been used to predict the liquefaction potential of soil strata, [12], [13]:

- (1) Evaluations based on a comparison of the stresses induced by an earthquake and the stress conditions causing liquefaction in cyclic laboratory tests on soil samples.
- (2) Empirical methods based on measurements of in situ soil strength and observations of field performance in previous earthquakes.

Unfortunately, liquefaction assessments based on laboratory tests are hindered by limitations in the ability of laboratory equipment to reproduce field stress conditions in small soil samples and disturbance of field samples is nearly impossible to avoid and very difficult to quantify in laboratory tests, [12].For this reason, empirical methods based on in situ penetration tests are favored for engineering assessments of liquefaction potential.

### 5.1 Evaluation of Cyclic Stress Ratio (CSR)

Seed and Idriss formulated the following equation for the calculation of the cyclic stress ratio (CSR), and this equation is still the most widely used empirical method, [10]:

$$\text{CSR} = \frac{\tau_{\text{av}}}{\sigma'_{\text{vo}}} = 0.65 \frac{a_{\text{max}}}{g} * \frac{\sigma_{\text{vo}}}{\sigma'_{\text{vo}}} * r_d \quad (2)$$

where:

$\tau_{\text{av}}$  = average cyclic shear stress induced by design ground motion,

$\sigma'_{\text{vo}}$  = initial vertical effective stress at the depth under consideration in static condition,

$\sigma_{\text{vo}}$  = initial vertical total stress at the depth under consideration in static condition,

$a_{\text{max}}$  = peak horizontal acceleration at the ground surface generated by the earthquake,

$r_d$  = stress reduction coefficient.

$g$ =gravity acceleration.

The NCEER workshop recommended the following equations for routine practice and noncritical projects, [7]:

$$r_d = 1.0 - 0.00765z \text{ for } z \leq 9.15\text{m} \quad (3a)$$

$$r_d = 1.174 - 0.0267z \text{ for } 9.15\text{m} < z \leq 23\text{m} \quad (3b)$$

$$r_d = 0.744 - 0.008Z \text{ for } 23 \text{ m} < z \leq 30 \text{ m} \quad (3c)$$

$$r_d = 0.50 \quad \text{for } z > 30 \text{ m} \quad (3d)$$

### 5.2 Evaluation of Cyclic Resistance Ratio (CRR)

Empirical methods for the evaluation of the CRR commonly employ the following field tests: the standard penetration test (SPT), the cone penetration test (CPT), shear wave velocity measurements, and the Becker penetration test (BPT), [8]. The SPT and CPT methods are generally preferred because of the more extensive database and past experience, but the other tests maybe applied at sites underlain by gravelly sediment or where access by large equipment is limited. In this research the evaluation of CRR is based on SPT.

### 5.3 CRR Evaluation methods based on Standard Penetration Test (SPT)

#### 5.3.1 NCEER (1997) and Vancouver(2007) methods

These two methods, [7], [8], are very similar expect that in Vancouver Task Force Report a  $K_\sigma$  parameter is multiplied in CRR7.5. The  $K_\sigma$  factor is calculated from the following formula:

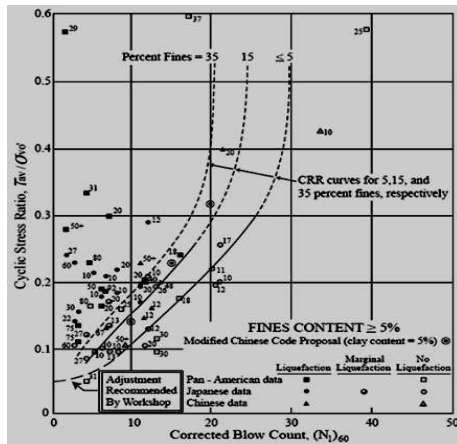
$$K_\sigma = \left( \frac{\sigma_{\text{vo}}}{P_a} \right)^{f-1} \quad (4)$$

Where  $P_a$  is atmospheric pressure in the chosen units and  $f$  depends on relative density ( $D_r$ ) and given by:

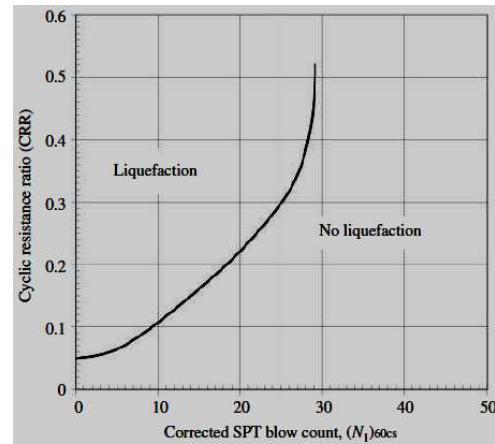
$$f = 1 - 0.005 * D_r \quad \text{for } 40\% < D_r < 80\% \quad (5)$$

In these methodologies, CRR7.5 is a function of depth corrected SPT blow counts  $(N_1)_{60}$  for clean sand (fines content less than 5 percent). For sands containing more fines content, more corrections will be applied on  $(N_1)_{60}$  (as shown in the following steps). The CRR7.5 curve proposed by the methodologies based on  $(N_1)_{60}$  are shown in Fig. 3:

Step 1: Corrections to overburden stress and various SPT equipment, more details were reported by Youd et al. [11], to account for the effect of overburden stress and various equipment used for SPT.



(a) Liquefaction Case Histories, [14]



(b) fines  $\leq 5\%$ , (from [2], [11])

Figure 3. SPT Clean sand Based Curve for Magnitude 7.5 Earthquake

The equation proposed by Thomas F. Blake recommended by NCEER Workshop (1997) for clean sand curve, as shown in Fig. 4, is used. This equation is valid for  $(N_1)_{60cs} \leq 30$ .

Step 2: Corrections to fines content. The corrected  $(N_1)_{60}$  is further corrected for the fines content (FC) in the soil. The following equations were developed by I.M. Idriss with the assistance of R.B. Seed, [11]:

$$(N_1)_{60cs} = \alpha + \beta(N_1)_{60} \quad (6)$$

where:

$(N_1)_{60cs}$  = the  $(N_1)_{60}$  for equivalent clean sand;  $(N_1)_{60cs}$  is used in Fig. 3 to find the CRR under magnitude 7.5 earthquakes,

$(N_1)_{60}$  = corrected SPT blow count to overburden stress and various SPT equipment

$\alpha$  and  $\beta$  = coefficients determined from the following relationships (Equations (7) and (8)):

$$\alpha = 0 \quad \text{for} \quad FC \leq 5\% \quad (7a)$$

$$\alpha = e^{\left(1.76 - \left(\frac{190}{FC^2}\right)\right)} \quad \text{for} \quad 5\% < FC < 35\% \quad (7b)$$

$$\alpha = 5 \quad \text{for} \quad FC \geq 35\% \quad (7c)$$

$$\beta = 1 \quad \text{for} \quad FC \leq 5\% \quad (8a)$$

$$\beta = \left(0.99 + \frac{FC^{1.5}}{1000}\right) \quad \text{for} \quad 5\% < FC < 35\% \quad (8b)$$

$$\beta = 1.2 \quad \text{for } FC \geq 35\% \tag{8c}$$

Step 3: Magnitude scaling factors (MSFs): A magnitude scaling factor (MSF) is used to correct the factor of safety (FS) when the earthquake magnitude is not 7.5:

$$FS = \frac{CRR_{7.5}}{CSR} * MSF \tag{9}$$

Where  $CRR_{7.5}$  is the cyclic resistance ratio for a magnitude 7.5 earthquake. There are several methods for MSF determination. One of them is that recommended by NCEER,[7]:

$$MSF = (7.5 / M)^{2.56} \tag{10}$$

The NCEER workshop summarized the MSFs proposed by various investigators as shown in Fig. 4, [7].

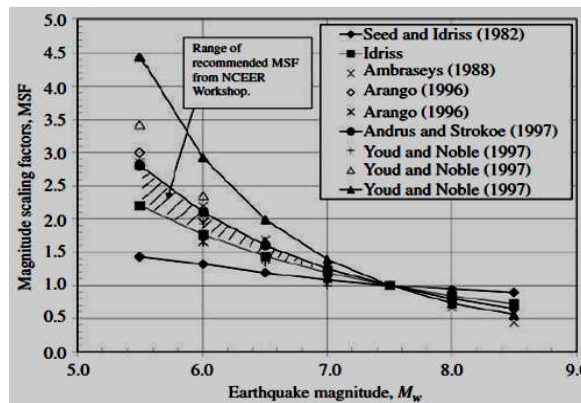


Figure 4. MSF derived by various investigators. (Reproduced from [15])

### 6.3.2 Idriss and Boulanger (2004)

The correlation between the cyclic resistance ratio (CRR) adjusted to  $M = 7.5$  and  $\sigma'_v = 1$  atm and the equivalent clean sand  $(N_1)_{60cs}$  value for cohesionless soils, as developed by Idriss and Boulanger is shown in Equation (11).

$$CRR_{M=7.5, \sigma'_v = 1 \text{ atm}} = e^{\left( \frac{(N_1)_{60cs}}{14.1} + \frac{(N_1)_{60cs}}{126} - \frac{(N_1)_{60cs}}{23.6} + \frac{(N_1)_{60cs}}{25.4} - 2.8 \right)} \tag{11}$$

### 6.3.3 Japanese Bridge Code

This methodology is based on SPT blow counts and particle size distribution of sand.

$$0.05mm < D_{50} < 0.6mm \rightarrow CRR_1 = 0.0882 \sqrt{\frac{N_{1(60)}}{\sigma'_v + 0.7}} + 0.255 \log \frac{0.35}{D_{50}} + R_3 \tag{12}$$

$$0.6mm < D_{50} < 2mm \rightarrow CRR_1 = 0.0882 \sqrt{\frac{N_{1(60)}}{\sigma'_v + 0.7}} - 0.05 \tag{13}$$

Where:

$$Fc < 40\% \rightarrow R_3 = 0$$

$$Fc \geq 40\% \rightarrow R_3 = 0.004Fc - 0.16$$



$D_{50}$  : particle size corresponding to 50 percent passing

$F_c$  : percent fines content passing sieve #200 (clay and silt)

In this research, the methods adopted for liquefaction assessment are NCEER [7], Vancouver [7], Idriss and Boulanger[16] and Japanese Bridge Code.

## 6.4 Post-Liquefaction

Liquefaction can dramatically alter the amplitude and frequency content of ground surface motions. As the buildup of excess pore pressure causes a layer of liquefiable soil to soften, ground surface displacements may increase even when ground surface accelerations decrease. Ground oscillations may produce chaotic permanent movement of fractured blocks of surficial soils, [17]. The occurrence of liquefaction at depth beneath a flat ground surface can decouple the liquefied soils from the surficial soils and produce large, transient ground oscillations. The surficial soils are often broken into blocks separated by fissures that can close during earthquake. Ground waves with amplitude of up to several feet have been observed during ground oscillation, but permanent displacements are usually small,[17]. In this research lateral spreading and settlement of the soil will be investigated.

### 6.4.1. Lateral Displacements

Liquefaction-induced lateral spreading of sloping ground and near waterfronts is a major cause of earthquake damage to deep foundations, [17]. Earthquake case histories in the US, Turkey and other countries, have shown damage to buildings, bridges, port facilities and other pile-supported structures. Effects include cracking and rupture of piles at both shallow and deep elevations, rupture of pile connections, and permanent lateral and vertical movements and rotations of pile heads with corresponding effects on the superstructure. Thus, the studying of liquefaction-induced lateral spreading is of interest in soils susceptible to liquefaction and of great interest when these soils have located near the water sources (rivers, lakes, etc.). In this paper, the liquefaction-induced lateral spreading is estimated using Zhang, Robertson and Brachman method, [18]. This approach can be applied to obtain preliminary estimates of the magnitude of lateral displacements associated with a liquefaction-induced lateral spread. This method is essentially based on estimating maximum cyclic shear strain of each layer during and after liquefaction which is estimated from safety factor against soil liquefaction (FS) and relative density of soil ( $D_r$ ), when  $D_r$  can be correlated from SPT or equivalent SPT blow counts as illustrated in Fig. 5. Then, the Lateral Displacement Index (LDI) is calculated from Equation14 as follows, [18]:

$$LDI = \int_0^{Z_{max}} \gamma_{max} dz \quad (14)$$

Where  $\gamma_{max}$  is the maximum shear strain in each layer induced by cyclic load, and  $dz$  is depth interval at each test.

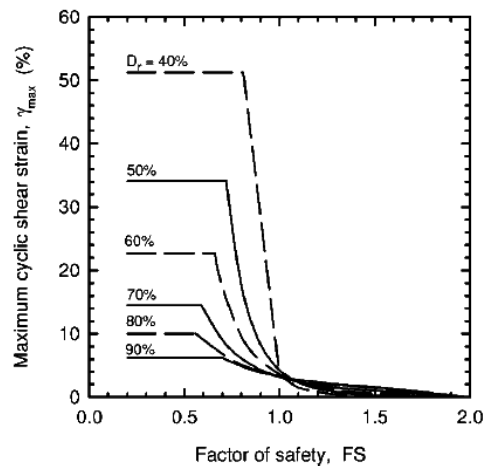


Figure 5. Maximum Cyclic Shear Strain for Post Liquefaction Lateral Displacement, [18]

#### 5.4.2 Reconsolidation Settlement

Post-liquefaction settlements occur during and after earthquake shaking. For level ground conditions the amount can be computed from the volumetric reconsolidation strains induced as the excess pore water pressures dissipate, [19]. Based on field experience during past earthquakes, the amount of volumetric strain depends on penetration resistance and the CSR applied by the design earthquake. Curves proposed by Ishihara and Yoshimi, [19], are shown in Fig. 7 and indicate that volumetric reconsolidation strains can range between about 4.5% for very loose sand to 1% for very dense sands. These curves are recommended for estimating post-liquefaction settlements.

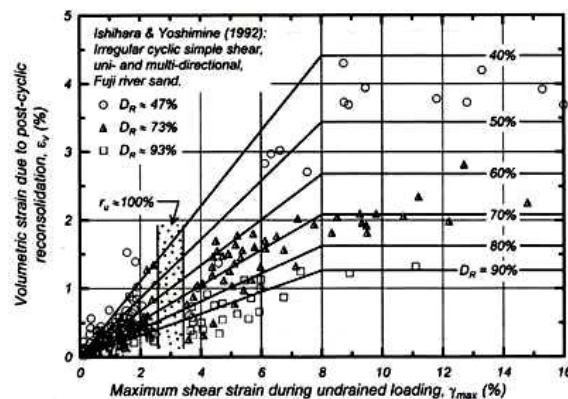


Figure 7. Volumetric Reconsolidation Strains as a Function of Maximum Shear Strain and Relative Density, [19]

## 7. Results And Discussions

The geodynamic configurations for Baghdad city and the observation of the Iraqi seismic acceleration map indicates that regions east of Tigris River have a high seismic acceleration (greater than 0.2g) while the region between Tigris and Euphrates Rivers experiences a lower acceleration (0.1-0.2g), [4]. Therefore; there is need for the assessment of liquefaction potential of the Holocene soils lie in this region. Hence, structures located especially on these areas that are not designed for earthquake forces are worst affected. Generally, Baghdad area has extensive tracts of loose to medium silty sand below a shallow layer of clay. Due to recurring seismic activity, there is a chance of the soil being subjected to liquefaction. With the collected bore-hole data, analysis for liquefaction is attempted using four SPT-based

liquefaction triggering procedures for cohesionless soils. The process of liquefaction evaluation had been performed depending on the values of acceleration that were obtained from the seismic acceleration map and earthquake magnitudes ranges from 4.5 to 7.1.

The results obtained from liquefaction analysis could be shown in Fig. 8 as safety factor variation with depth. The examination of the results in Fig.8 reveals that the soil in the seven sites have susceptibility to liquefaction in different degrees, depending on the seismic properties, soil condition and its geotechnical properties. This finding coincides with the thought that liquefaction occur in soils adjacent to rivers, lakes, bays and oceans, [17].In addition, it is observed that acceleration has highly effect on the soil susceptibility to liquefaction, while the Magnitude effect is very limited as shown in Fig.8. Moreover, it is found that site (S5) is the least susceptible to liquefaction since it has as a minimum  $(N1)_{60}$  greater than 15 blows at a depth of nearly 3m. This means that the soil needs larger acceleration to be prone to liquefaction. This behavior coincides with the description presented by Ohasaki, [20] which say that liquefaction is not a problem if the blow count from a standard penetration test exceeds twice the depth of the sample in meters.

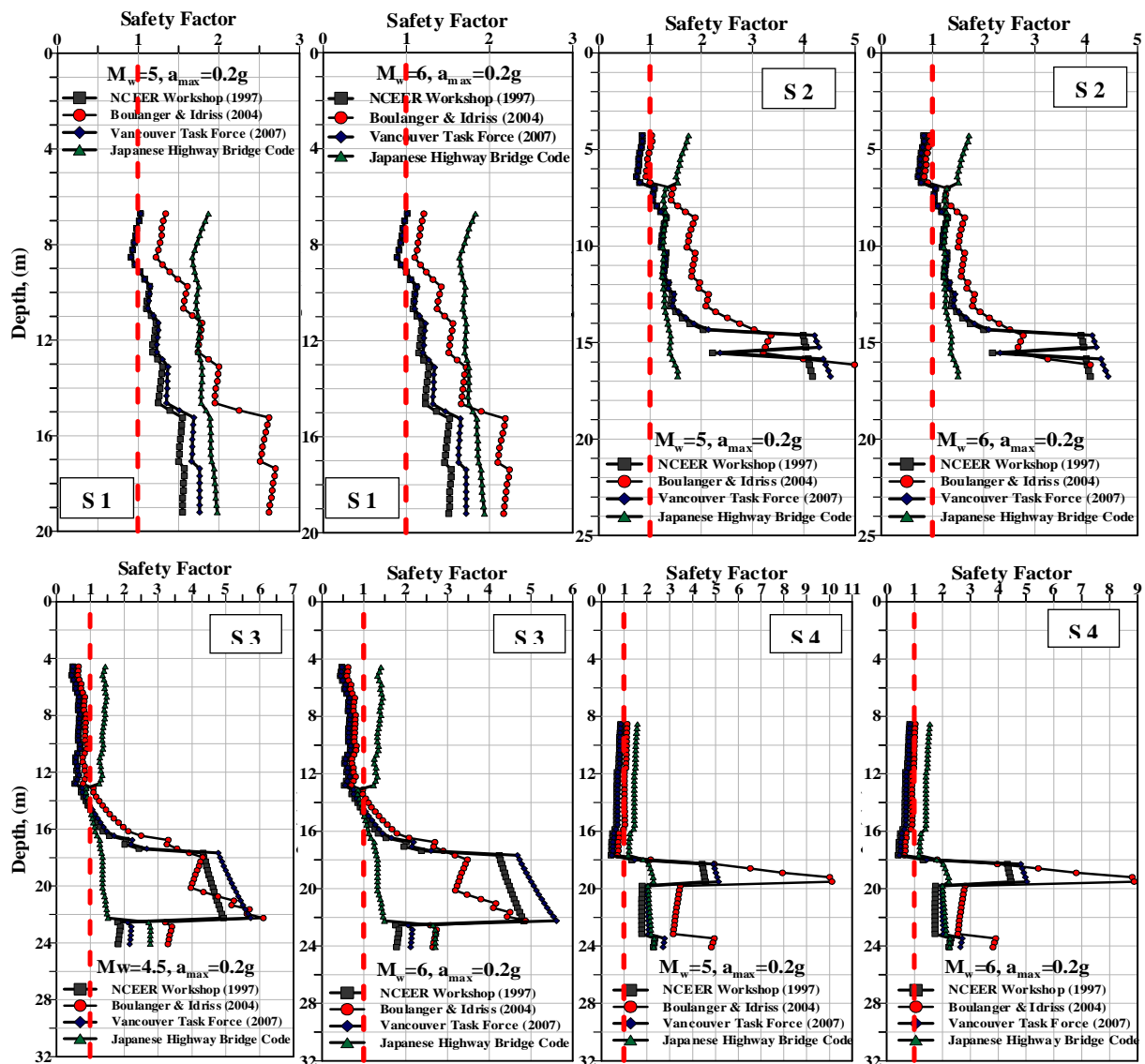


Figure 8. The Variation of Factor of Safety with Depth

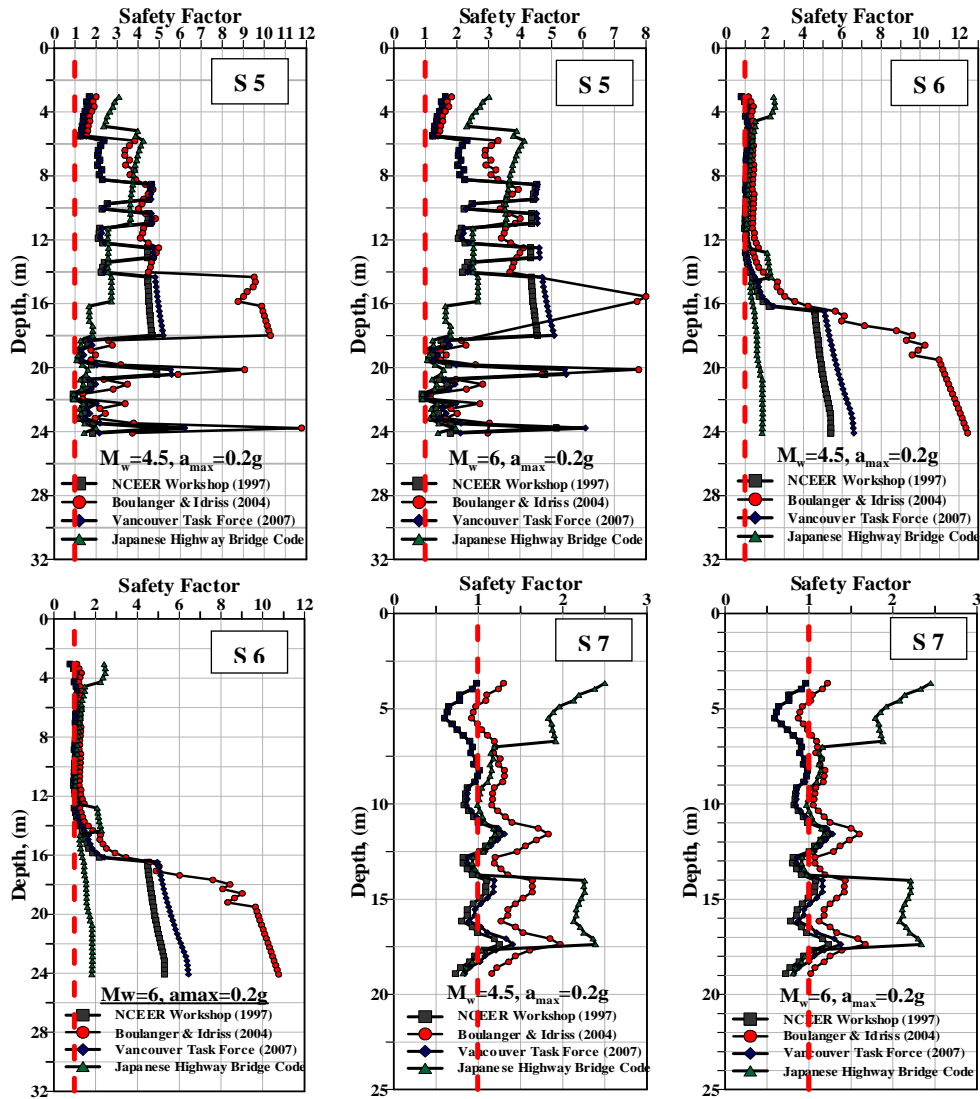


Figure 8. Continued

Also, it has been observed that there is some difference in results of liquefaction triggering procedures that were followed in analysis. The differences in safety factor values for different adopted methods, have been presented as contours of the ratio of safety factor determined by each method to the safety factor determined by NCEER procedure, i.e.  $FS_{I\&B}/FS_{NCEER}$ ,  $FS_{Vancouver}/FS_{NCEER}$ , and  $FS_{Japanese}/FS_{NCEER}$ . These contours for all sites can be shown in Fig.9. It is important to note that the mentioned methods are based on case histories data largely limited to depths less than 12m. For this range of depths, Idriss-Boulanger correlation gives CRR values that are generally within  $\pm 10\%$  of the results obtained using the NCEER procedure, [16]. The greatest contributors to these differences in the SF values obtained by these three procedures are the baseline triggering correlation and the  $K_\sigma$  relationships. The contours show that the differences in SF values tend to be negligible for Vancouver procedure, intermediate for Idriss and Boulanger procedure, and largest for the Japanese procedure. Thus, the assessment of liquefaction for Baghdad soil using Japanese procedure is not recommended.

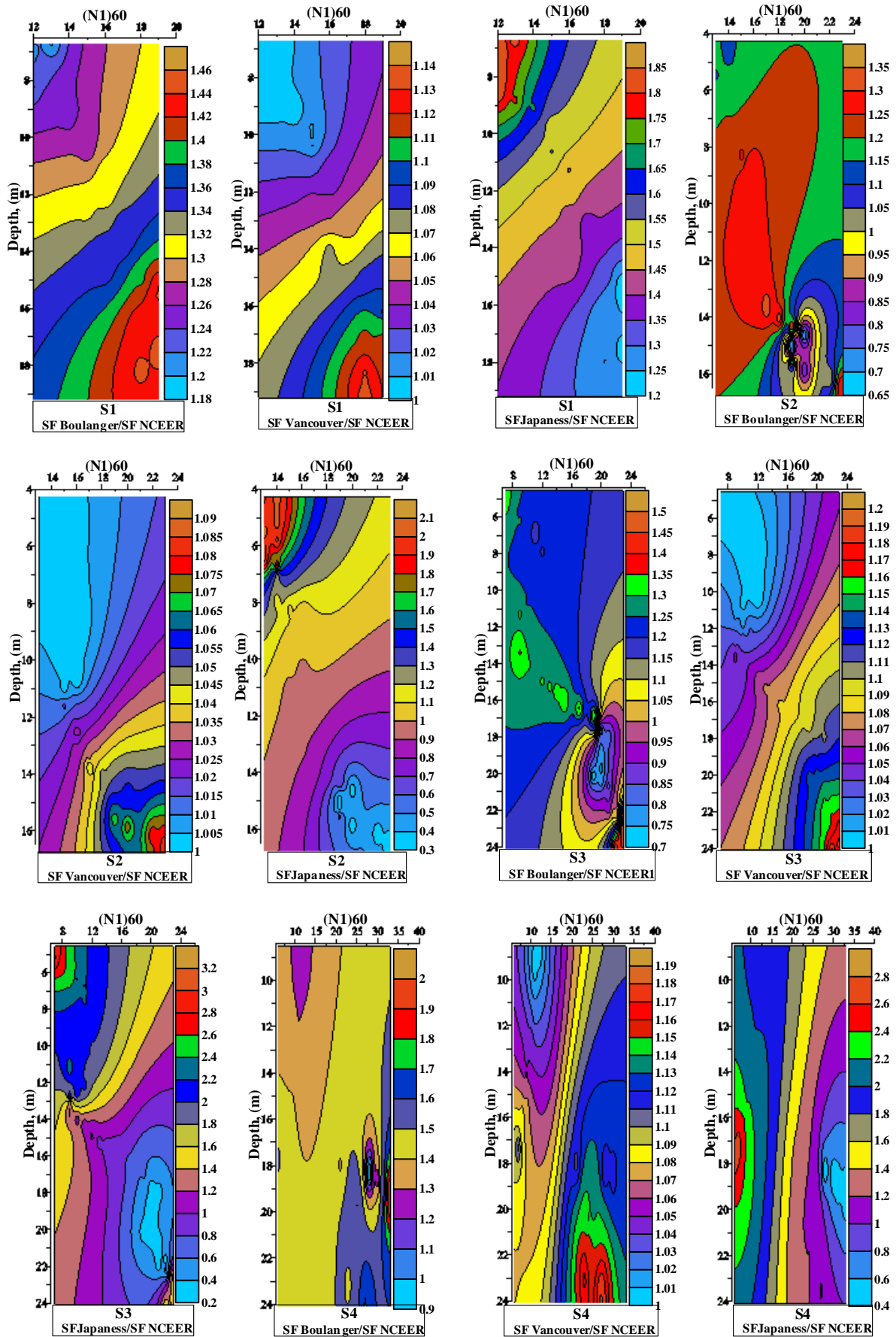


Figure 9. Comparison of Liquefaction Analysis Procedures of Idriss and Boulanger (2004) , Vancouver (2007) , Japanese Highway Code and NCEER (1997) for Mw= 6 and amax=0.2g



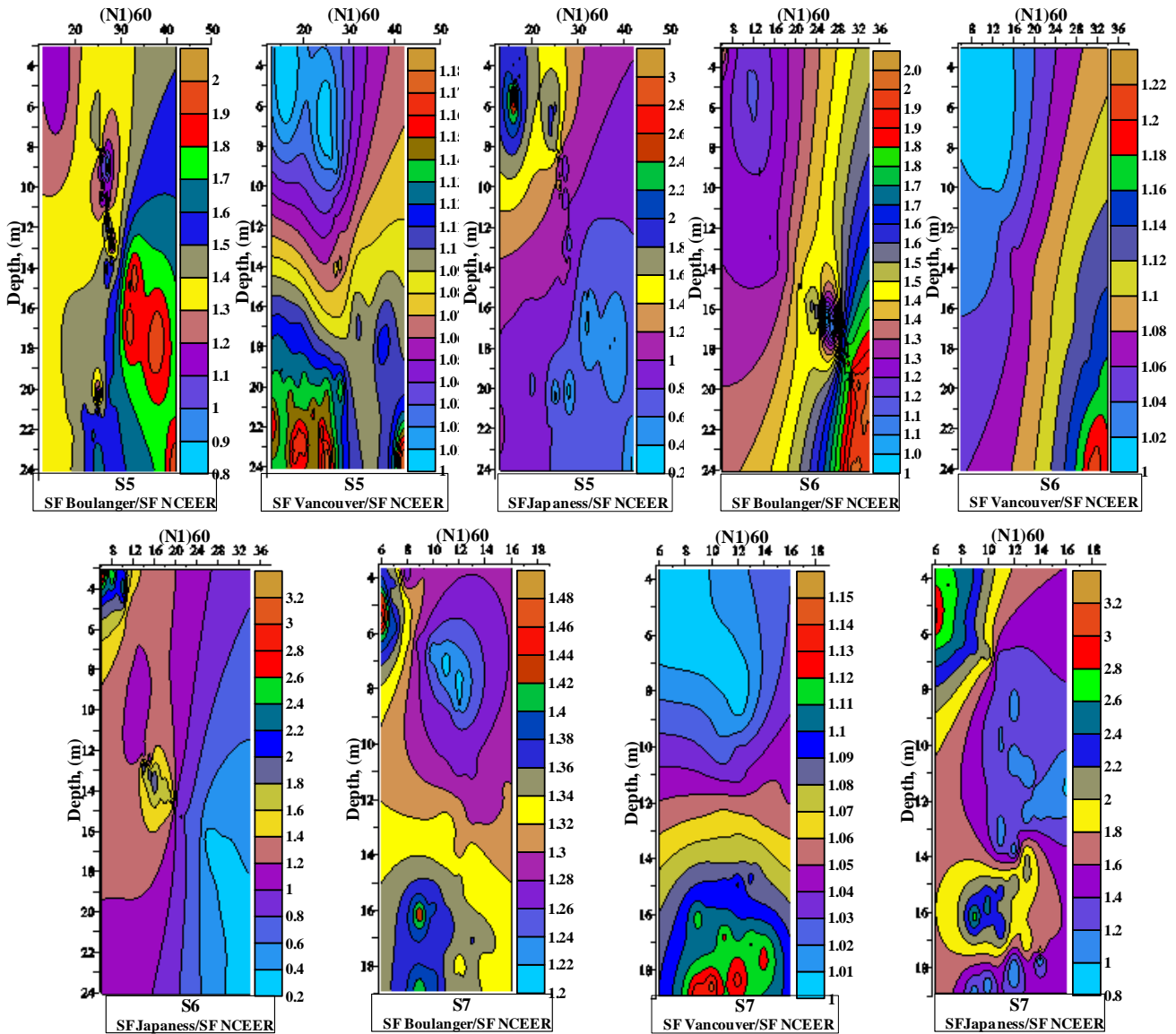


Figure 9. Continued

The seismic hazard analysis and the site characterization efforts are often the most important components of any probabilistic assessment of liquefaction hazards. Considerable differences in correlation procedures, especially for earth dams when depths of liquefiable zones may be considerable, may affect scores of \$Millions on yearly basis, [21].

Among the different procedures of liquefaction assessment, the 1996/1998 NCEER workshop was last general consensus of community, [11].

Fig. 10 shows the variation of thickness of liquefied layer which have been computed using different methods. These computations have been made at earthquake magnitude of 5.5 and 6 and acceleration of 0.2g and 0.25g for each magnitude. It is clear that, whenever the earthquake magnitude is greater the estimated thickness of the liquefied layer is greater. Also, it has been noticed that the thickness of the liquefied layer at  $a_{max} = 0.25g$  is greater than its value at  $a_{max} = 0.2g$  for the same earthquake magnitude. The increase in acceleration amplitude leads to reduce the soil resistance to liquefaction. The sites (S3, S4, and S7) revealed greater thickness of liquefied layers while the other sites (S1, S2, S5, and S6) exhibit lower values. This behavior is attributed to the geotechnical properties of each site such as relative density

(Dr) and initial confining stress. The loose soil is more susceptible to liquefaction than medium soil.

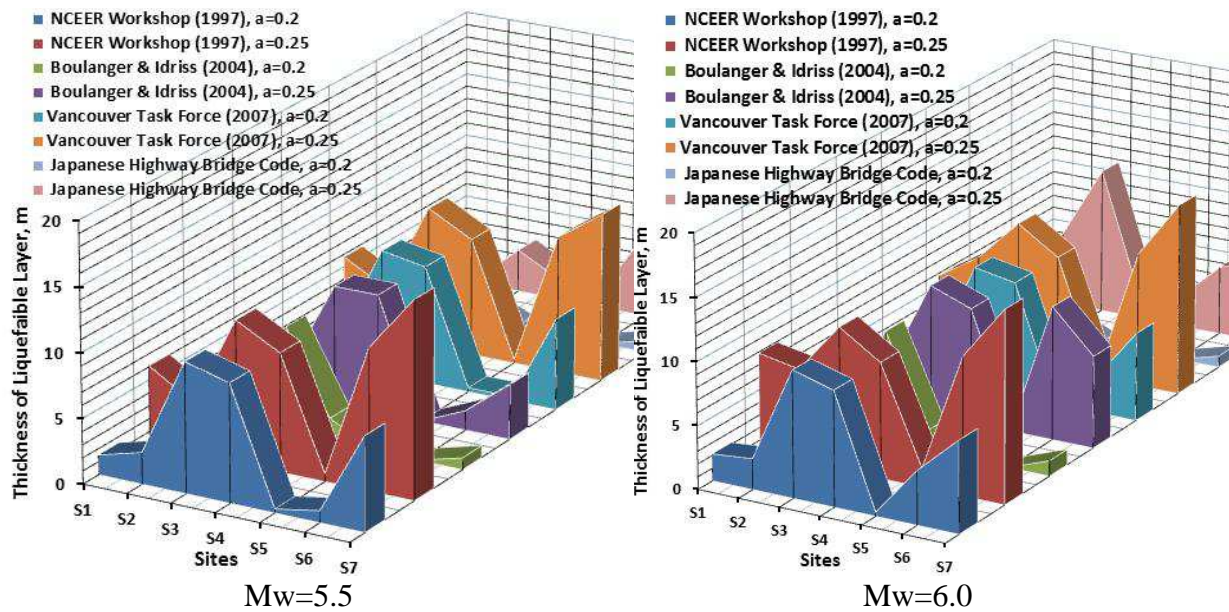


Figure 10. The Variation of Thickness of Liquefied Layer for all Sites Determined at (Mw = 5.5, 6 and  $a_{max}=0.2g$  and  $0.25g$ )

The liquefaction-induced lateral displacement index (LDI) and settlement of all sites which had been investigated in this paper are illustrate in Table 2. Throughout inspecting Table 2, the results of site S7 will attract the sight and interest. The results of site S7 represent the highest values of LDI and settlement. This may be attributed to the low relative density that Site S7 has in addition to its nearest location from Tigris River. The areas adjacent to rivers are most commonly prone to liquefy, [22].

Table 2. Lateral Displacement Index and Settlement for all Sites (Determined at  $a_{max}=0.2$ )

Property	Movement (cm)														
	site	S1	S2	S3	S4	S5	S6	S7	S1	S2	S3	S4	S5	S6	S7
Mw		5	6	5	6	5	6	5	6	5	6	5	6	5	6
LDI, [17]		0	0	6	6	5	3	3	2	0	0	4	3	70	69
Settlement, cm, [18]		0	0	3	3	3	2	2	1	0	0	2	1	15	14

The sites that studied in this paper lies along Tigris River have the same geologic origin (Quaternary Sediments that range in age from Pleistocene to Holocene). Therefore, a thought of using of all the results, which were obtained from liquefaction evaluation, in statistical analysis has been born. This analysis aims to find an appropriate mathematical model that expresses the relationship between a dependent variable (safety factor, FS) and a single independent variable (corrected SPT blows,  $(N1)60$ ). High level of correlation ( $0.84 \leq R \leq 0.96$ ) has been found between FS and  $(N1)60$ . The relation between these parameters is represented graphically as a chart to use for preliminary assessment of the liquefaction, as illustrated in Fig. 11. Hence, this chart is going to be a helpful tool in saving time and cost, for similar soils of comparable properties and conditions with that used in this paper, so as to

check soil susceptibility to liquefaction. Once the value of  $(N1)_{60}$  have known, the Safety factor (FS) can be estimated according to the design earthquake and seismic properties of the investigated area.

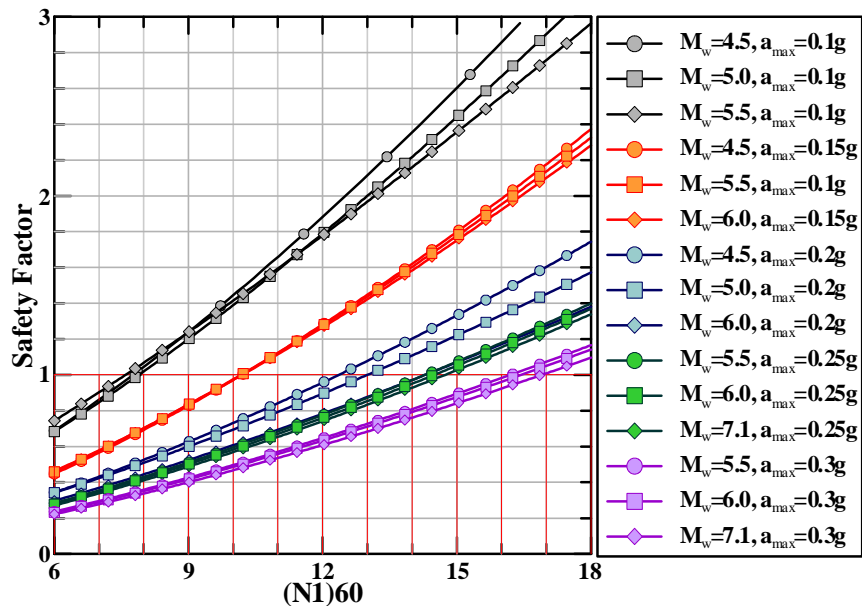


Fig. 11: Proposed Chart for Assessment of Liquefaction of Soil in Baghdad

## 8. Conclusions

The evaluation of liquefaction susceptibility of Baghdad soil in nature for engineering purposes is performed based on different empirical procedures using Standard Penetration Test results obtained by in-situ testing. The extensive investigation of susceptibility of Baghdad soil to liquefaction revealed the following conclusions:

1. The soils in the seven sites have susceptibility to liquefaction in different degrees, depending on the seismic properties, soil condition and its geotechnical properties.
2. It is observed that acceleration has highly effect on the soil susceptibility to liquefaction, while the Magnitude effect is very limited.
3. It has been observed that there is some difference in results of liquefaction triggering procedures that were followed in analysis. The greatest contributors to these differences in the SF values obtained by these three procedures are the baseline triggering correlation and the  $K_{\sigma}$  relationships. The contours show that the differences in SF values tend to be negligible for Vancouver procedure, intermediate for Idriss and Boulanger procedure, and largest for the Japanese procedure.
4. The NCEER (1997) Workshop, that has last general consensus of community, is recommended in assessment of liquefaction for Baghdad soil. While the Japanese procedure is not recommended.
5. The highest values of LDI and settlement were observed at site S7 which is the nearest site from Tigris River in this study.
6. With the results obtained in this study, an attempt is made to treat these results statistically. High level of correlation ( $0.84 \leq R \leq 0.96$ ) has been found between FS and  $(N1)_{60}$ . The relation between these parameters is represented graphically as a chart to use for

preliminary assessment of the liquefaction for Baghdad soil. This chart is going to be helpful tool in saving time and cost.

## 9. References

1. Alsinawi, S.A. (2001). "*Seismological Considerations of the Eastern Arab Region*". Proc.Euro-Mediterranean Seminar on Natural Environmental and Technological Disasters, Algiers.
2. Xiao, M. (2015). "*Geotechnical Engineering Design*". John Wiley & Sons, Ltd, United Kingdom.
3. Ambrassys, N. N. and Melville, C. P.(1982). "*A History of Persian Earthquakes*". Cambridge University Press.
4. Jassim, S. Z. and Goff, J. C. (2006). "*Geology of Iraq*". Dolin, Prague and Moravian Museum, Brno.
5. Ameer, S. A., M.L. Sharma, H.R. Wason and S. A. Alsinawi (2005). *Probabilistic Seismic Hazard Assessment for Iraq Using Complete Earthquakes Catalogue Files*. Pure and Applied Geophysics, Vol. 162, No. 5, pp. 951-966.
6. Iraqi Meteorological Organization and seismology (2013). Retrieved December 2, 2015, from <http://meteoseism.gov.iq/index.php?name=Pages&op=page&pid=168>.
7. NCEER Workshop (1997). Proceeding on Evaluation of Liquefaction Resistance of Soils. Nat. Ctr. for Earthquake Eng. Res., State Univ. of New York at Buffalo.
8. Vancouver Task Force Report (2007). Task Force Report, Geotechnical Design Guidelines For Buildings on Liquefiable Sites in Accordance with NBC 2005 for Greater Vancouver Region, May 8, 2007.
9. Idriss, I. M., and Boulanger, R. W. (2004). "*Semi-empirical Procedures for Evaluating Liquefaction Potential During Earthquakes*". Proc., 11<sup>th</sup> Int. Conf. on Soil Dynamics and Earthquake Engineering, and 3<sup>rd</sup> Int. Conf. on Earthquake Geotechnical Engineering, D. Doolin et al., eds., Stallion Press, Vol. 1, pp. 32–56.
10. Seed, H. B., and Idriss, I. M. (1971). *Simplified Procedure for Evaluating Soil Liquefaction Potential*. Journal of Soil Mechanics and Foundations Division, ASCE, Vol. 97, No. 9, pp. 1249–1273.
11. Youd, T., Idriss, I., Andrus, R., Arango, I., Castro, G., Christian, J., Dobry, R., Finn, W., Harder, L., Jr., Hynes, M., Ishihara, K., Koester, J., Liao, S., Marcuson, W., III, Martin, G., Mitchell, J., Moriwaki, Y., Power, M., Robertson, P., Seed, R., and Stokoe, K., (2001). *Liquefaction resistance of soils: Summary report from the 1996 NCEER and 1998 NCEER/NSF workshops on evaluation of liquefaction resistance of soils.* J. Geotech. Geoenviron. Eng., ASCE, Vol. 127, No. 10, pp. 817–833.
12. Seed, H. B. (1979). *Soil Liquefaction and Cyclic Mobility Evaluation for Level Ground during Earthquakes*. J. Geotech. Engrg. Div., ASCE, Vol. 105, No. 2, pp. 201–255.
13. Seed, H.B., Tokimatsu, K., Harder, L.F., and Chung, R.M., (1985). *The Influence of SPT Procedures in Soil Liquefaction Resistance Evaluations*. Journal of Geotechnical Engineering, ASCE, Vol. 111, No. 12, p. 1425-1445.
14. Youd and Idress,(2001). *Liquefaction Resistance of Soils: Summary Report From The 1996 Nceerand 1998 Nceer/Nsf Workshops on Evaluation of Liquefaction Resistance of Soils*. Journal of Geotechnical and Geoenvironmental Engineering, Vol. 127, No. 4.

15. Youd, T. L., and Noble, S. K. (1997). "*Magnitude scaling factors*". Proc., NCEER Workshop on Evaluation of Liquefaction Resistance of Soils, Nat. Ctr. for Earthquake Engrg. Res., State Univ. of New York at Buffalo, pp.149–165
16. Idriss, I. M. and Boulangor, R. W. (2010). "*SPT-Based Liquefaction Triggering Procedures*". Report No. UCD/CGM-10-02, Center for Geotechnical Modeling Department of Civil and Environmental Engineering University of California Davis, California.
17. Kramer, S.L. (1996). "*Geotechnical Earthquake Engineering*". Prentice Hall, Upper Saddle River.
18. Zhang, G., Robertson, P., and Brachman, R. (2004). "*Estimating Liquefaction-Induced Lateral Displacements Using the Standard Penetration Test or Cone Penetration Test*", Journal of Geotechnical and Geoenvironmental Engineering, Vol. 130, No. 8, pp. 861-87.
19. Ishihara, K., and Yoshimine, M. (1992). "*Evaluation of Settlements in Sand Deposits Following Liquefaction during Earthquakes*". Soils and Foundations, Vol. 32, No. 1, pp. 173–188.
20. Ohasaki, Y. (1970). "*Effects of sand compaction on liquefaction during the Tokachioki earthquake*". Soils and Foundations, Vol. 10, No. 2, pp.112-128.
21. EERI (2010). EERI Ad Hoc Committee Report on Soil Liquefaction During Earthquakes, T.D. O'Rourke Thomas R. Briggs Professor Cornell University.
22. Day, R.W. (2006). "*Foundation Engineering Handbook*". The McGraw-Hill Companies, Inc.